

Classical orbit bifurcation and quantum interference in mesoscopic magnetocconductance

J. Blaschke and M. Brack

Institut für Theoretische Physik, Universität Regensburg, D-93040 Regensburg, Germany

(October 1, 2018)

We study the magnetoconductance of electrons through a mesoscopic channel with antidots. Through quantum interference effects, the conductance maxima as functions of the magnetic field strength and the antidot radius (regulated by the applied gate voltage) exhibit characteristic dislocations that have been observed experimentally. Using the semiclassical periodic orbit theory, we relate these dislocations directly to bifurcations of the leading classes of periodic orbits.

03.65.Sq, 73.20.Dx, 73.23.Ps

Since it has become feasible to laterally confine a two-dimensional electron gas (2DEG) on length scales considerably smaller than the mean-free path of the electrons, the connection between classical and quantum mechanics has gained increasing renewed interest. Therefore, many experimental and theoretical investigations have recently been focused on the onset of quantum interference effects in mesoscopic ballistic devices. A well-adapted theoretical tool for this regime is the semiclassical approach that approximates quantum mechanics to leading orders in \hbar . It is conceptually quite remarkable because it links quantum interference effects to purely classical phase-space dynamics. The so-called trace formula, originally developed by Gutzwiller [1] for the density of states of a system with only isolated orbits in phase space, has been extended to systems with continuous symmetries [2,3] (see Ref. [4] for further literature) and for other physical properties such as conductance [5,6] or magnetic susceptibility [7,8]. Many quantum interference effects observed in mesoscopic systems could successfully be explained by the interference of a few classical periodic orbits, such as the Shubnikov-de-Haas oscillations of the free 2DEG [5,6], the magnetoconductance oscillations of a 2DEG in an antidot superlattice [5,6,9,10] or a large circular quantum dot [11], or the current oscillations in a resonant tunneling diode (RTD) [12]. (See Ref. [4] for examples from nuclear and metal cluster physics.)

Real physical systems are usually neither integrable nor fully chaotic, but exhibit mixed phase-space dynamics. Upon variation of an external parameter (e.g., deformation, magnetic field strength, or energy), bifurcations of periodic orbits typically occur, whereby new orbits are born and/or old orbits vanish. In the RTD [12], period-doubling bifurcations were found to be responsible for a period doubling in the oscillations of the observed I-V curves. In superdeformed nuclei [13] and in the elliptic billiard [14], period-doubling bifurcations dominate the

quantum shell structure locally through new-born orbit families whose amplitudes are of relative order $1/\hbar$. Here we discuss a different mechanism through which orbit bifurcations manifest themselves in the magnetoconductance of a mesoscopic device, a narrow channel with central antidots. We present a semiclassical interpretation of dislocations in the conductance maxima as functions of antidot diameter and magnetic field strength and relate them to bifurcations of the leading classes of periodic orbits. We will show that their effect is neither due to their leading order in \hbar nor to period doubling, but to a subtle interference of different orbit generations with comparable periods.

For the semiclassical description of the conductance we follow the approach of Refs. [5,6]. The smooth part of the conductance G_{xx} (in the direction x of the electric current) can be described by the classical Kubo formula, whereas its oscillating part δG_{xx} is approximated in terms of periodic orbits (po):

$$\delta G_{xx} = \frac{1}{\ell^2} \frac{4e^2}{h} \sum_{po} C_{xx} \frac{R_{po}(\tau_\beta) F_{po}(\tau_s)}{|\text{Det}(\tilde{M}_{po} - \mathbf{1})|^{1/2}} \cos \left(\frac{S_{po}}{\hbar} - \mu_{po} \frac{\pi}{2} \right). \quad (1)$$

Here S_{po} is the action (evaluated at the Fermi energy E_F), μ_{po} the Maslov index, and \tilde{M}_{po} the stability matrix of each periodic orbit [1]. The temperature T is included in the factor $R_{po}(\tau_\beta) = (T_{po}/\tau_\beta)/\sinh(T_{po}/\tau_\beta)$ involving the (primitive) time period T_{po} and the scattering time $\tau_\beta = \hbar/(\pi kT) \approx 2.4 * 10^{-11}$ s. Damping due to a finite mean free path is given by $F_{po}(\tau_s) = e^{-T_{po}/(2\tau_s)}$, where $\tau_s = m^* \mu / e \approx 3.8 * 10^{-11}$ s is the scattering time extracted from the experimental mobility μ . $\ell \simeq 1\mu\text{m}$ is the characteristic length of the active region, and C_{xx} is the velocity-velocity correlation function of the periodic orbit, defined by

$$C_{xx} = \int_0^\infty dt e^{-t/\tau_s} \int_0^{T_{po}} d\tau v_x(\tau) v_x(t + \tau). \quad (2)$$

Eq. (1), as well as the standard trace formulae for the density of states, diverges at bifurcation points where two (or more) stationary points of the action coalesce and the stationary-phase approximation [1] in the trace integral leads to $\text{Det}(\tilde{M}_{po} - \mathbf{1}) = 0$. This can be locally overcome by expanding the action into higher-order normal forms [15]. The simultaneous requirement of asymptotically reaching the Gutzwiller amplitudes far from the bifurcation points leads to uniform approximations which were

developed systematically by Sieber and Schomerus [16]. At the critical points the amplitudes are increased by a factor $\hbar^{-\delta}$, where δ depends on the type of the bifurcation [17]. In the classical limit $\hbar/S \rightarrow 0$, bifurcations therefore may dominate the quantum oscillations. In real systems \hbar/S is, however, finite so that the other prefactors in the trace formula may compensate the factor $(S/\hbar)^\delta$ to a degree that depends on the specific system. Note that the uniform approximations of Refs. [16] are restricted to isolated bifurcations; a general treatment of bifurcations of higher codimension (i.e., bifurcations of bifurcations) is still lacking [18]. We employ a slightly modified version of the uniform treatment of Ref. [16], incorporating the discrete symmetries of the present system. To include effects of complex ‘ghost orbits’ not available in our calculations, we use the local approximation of their contribution derived from the numerical information at the bifurcation points. (For the technical details we refer to a forthcoming extended publication.)

The device investigated here consists of electrostatic gates confining a high-mobility 2DEG in a GaAs/GaAlAs heterostructure (see Fig. 1). The 2DEG was 82nm beneath the surface, its electron density was $\approx 3.47 * 10^{15} \text{ m}^{-2}$, and the mobility about $100 \text{ m}^2 \text{ V}^{-1} \text{ s}^{-1}$. Four metallic gates are used to define a long, narrow channel ($5 \mu\text{m} \times 1 \mu\text{m}$). These and two circular antidot gates are contacted individually. Details about the device are presented in [19–21] and the references cited therein. All measurements were taken at $T \approx 100 \text{ mK}$ using standard low-excitation AC techniques.

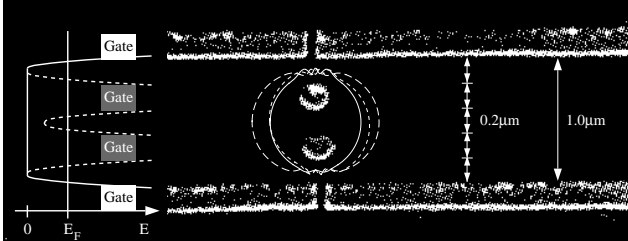


FIG. 1. SEM photograph of the gate structure [19] (without contacts). Left: Model potential used for the calculations. Center: Typical periodic orbits. Note that some of them break the discrete symmetries of the potential.

The dots in Fig. 2(a) show the experimental maximum positions of δG_{xx} as functions of magnetic field B and antidot gate voltage V_g [21]. The nearly equally spaced maxima and their shift to higher B for decreasing antidot diameter can be understood in analogy to the Aharonov-Bohm (AB) effect, if the AB ring is identified with cyclotron orbits around the antidots. Extracting the effective area from the experimental data yields a diameter between $0.76 \mu\text{m}$ and $0.86 \mu\text{m}$, which is consistent with the device dimensions. The dislocations of the peak positions (see the boxes in Fig. 2), however, cannot be understood within this simple picture. They have

been qualitatively reproduced in a quantum calculation by Kirczenov *et al.* [21].

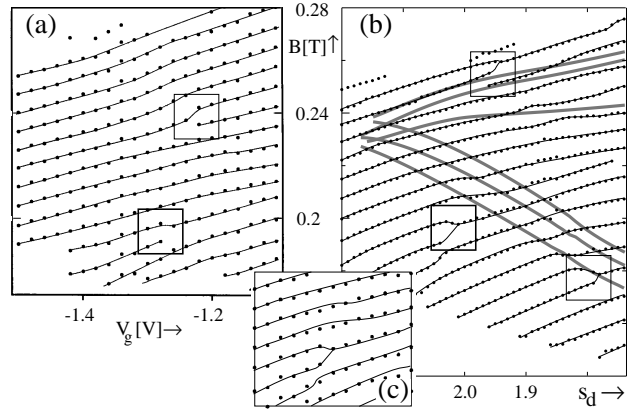


FIG. 2. Maximum positions of δG_{xx} versus magnetic field strength and gate voltage (antidot size). (a) Dots from experiment, connected with lines to guide the eye (reproduced with kind permission of the authors [21]). (b) Semiclassical results. The gray-shaded lines correspond to the loci of orbit bifurcations. (c) Behavior near a dislocation (see text). Dots: experiment; lines: semiclassical results.

Our objective is to decide if these dislocations and the variation of the spacings between the maxima can be understood semiclassically (which was doubted in Refs. [19,21]). For the effective one-electron model potential we follow essentially Kirczenov *et al.* [21] who assumed a parabolic shape $V(r) = E_F [r/a_0 - (1+s)]^2$ for $r < a_0(1+s)$ and $V(r) = 0$ otherwise. Here r denotes the distance to the gate, and a_0 is the length scale over which the potential falls from E_F to 0, i.e., the diffuseness of the potential. s is a dimensionless parameter modeling the depletion width around the gates. We use $a_0 = 0.05 \mu\text{m}$ and $s = s_c = 1$ for the gates defining the channel throughout this paper. The depletion width s_d of the antidot gates is varied between 1.5 and 2.2. According to Ref. [21], this corresponds to an effective antidot diameter of $\approx 0.35 \mu\text{m}$ to $0.42 \mu\text{m}$.

Following Eckhardt and Wintgen [22], we numerically integrate simultaneously the classical equations of motion and the reduced (2D) stability matrix M . The orbits are converged to periodicity using the information provided by M . They are followed through varying B fields and antidot diameters using an adaptive extrapolation scheme. We find a large variety of distinct periodic orbits, many of them breaking the symmetry of the potential. Some typical examples are shown in Figs. 1 and 3. We have included over 60 orbits (not counting their symmetry-related partners). Their actions, velocity-velocity correlation functions and periods were evaluated numerically. The Maslov index was determined similarly to Ref. [22].

Since the orbit bifurcations are of leading order in \hbar , we now want to check if they have an increased influence on the amplitude of the conductance oscillations.

In Fig. 3(a) we show the quantity $\text{Tr}\tilde{M}$ of four typical periodic orbits (shown to the right) taking part in two successive bifurcations (where $\text{Tr}\tilde{M} = 2$) under variation of the magnetic field strength B . The left one is a tangent bifurcation, the right one a pitchfork bifurcation.

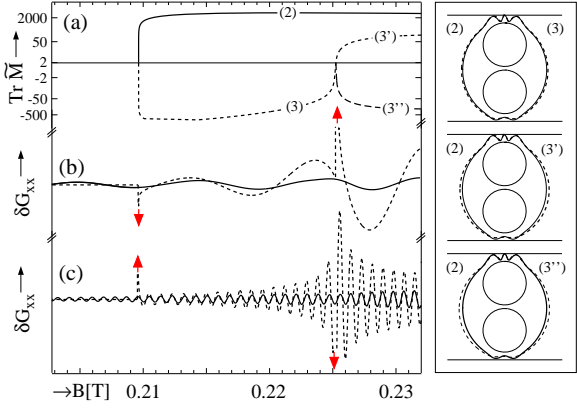


FIG. 3. Right: Four typical orbits (2: solid line; 3, 3': dashed lines) involved in two successive bifurcations. Left: (a) Trace $\text{Tr}\tilde{M}$ (note the nonlinear scale) versus magnetic field B . (b) Contribution of all orbits to δG_{xx} . Dotted line: Gutzwiller; solid line: uniform approximation. (c) Same as (b) but with actions scaled to be 10 times larger.

In Fig. 3(b), the contribution of these orbits to the conductance is plotted. The dotted line gives the result of the trace formula Eq. (1). The amplitudes are diverging (arrows!) at the bifurcations. The uniform approximation (solid line) removes the divergences. Fig. 3(c) represents the corresponding data for a system scaled to have 10 times larger actions, thus being closer to the semiclassical limit. It is important now to note that the amplitudes in the uniform approximation are nearly constant over the bifurcations. We have thus shown that the bifurcations have no locally dominant influence on the conductance of the present system [23].

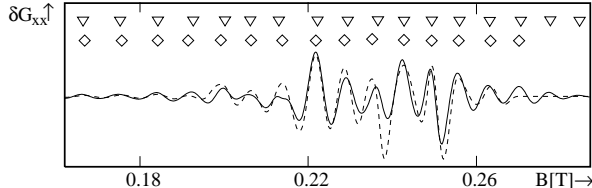


FIG. 4. δG_{xx} using Eq. (1) (dashed line) and the uniform approximation (solid line) after a convolution over B . Maxima are marked by boxes and triangles, respectively.

Having established this result, we can further simplify our semiclassical treatment. Whereas for individual orbits a uniform treatment of the bifurcations is vital, their influence becomes smaller if a larger number of orbits is included. This is demonstrated in Fig. 4, where the total δG_{xx} has been calculated for $s_d = 1.86$ including all relevant (~ 60) periodic orbits. The solid line shows the result of the uniform approximation, whereas the dotted

line corresponds to the standard Gutzwiller approach. To remove the spurious divergences in Eq. (1) (and those due to bifurcations of higher codimension in the uniform approach), we have additionally convoluted δG_{xx} over the magnetic field B (cf. Ref. [24]). The results are very similar [25]. In particular, the maximum positions are practically identical. In the following, we therefore use simply Eq. (1) with an additional convolution over B .

The semiclassical result for the maximum positions in δG_{xx} is shown in Fig. 2(b). We do not obtain a detailed quantitative agreement with the experimental data, since no effort has been made to optimize the model potential. Qualitatively, however, all features of the observed phase plot in Fig. 2(a) are reproduced. The spacing of the maxima will be analyzed in our extended publication, where we also compare our results to those of quantum calculations, optimize the potential $V(r)$ and discuss the scaling properties of our results. Presently we want to concentrate on the dislocations (see the boxes in Fig. 2), which are clearly reproduced in our approach. The semiclassical description even reproduces quantitatively the local behavior at the dislocations. This is shown in Fig. 2(c) that corresponds to the heavy boxes in Figs. 2(a) and (b). The points give the experimental maximum positions; the lines correspond to the semiclassical results (with slightly shifted but unscaled values of s_d and B).

To understand the semiclassical origin of these dislocations, we consider for the moment a model system with only 7 closely related orbits. The inserts in Fig. 5(b) show $\text{Tr}\tilde{M}$ of these orbits versus B for two different antidot diameters. With decreasing s_d , new orbits are born at the bifurcations. We classify the orbits in a grandparent, a parent and a child generation, depending if they are offsprings of orbit 1, 2, or 3, respectively. All members within a generation behave nearly identically, thus

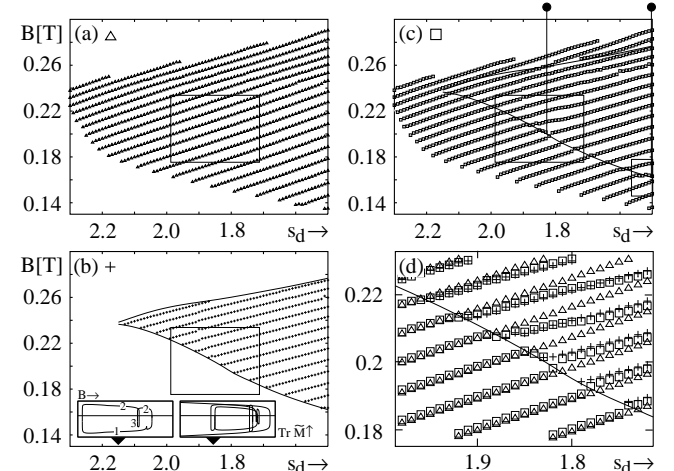


FIG. 5. Maximum positions due to different orbit generations: (a) grandparents, (b) children, (c) all generations. (d) Blow-up from (a)-(c): the maxima of the total δG_{xx} (squares) follow the maxima of the children (crosses), where these exist, and those of the grandparents (triangles) otherwise. Heavy lines indicate the loci of bifurcations in the (s_d, B) plane.

justifying our classification. The contribution of the grandparent and the child orbits to the conductance is shown in Figs. 5(a) and (b), respectively. The behavior of each generation is in complete agreement with the simple AB picture discussed above, but the effective areas and their dependence on B are different. The children have a larger semiclassical amplitude than the grandparents, thus dominating the conductance. Therefore the maxima of the total δG_{xx} closely follow the children's wishes where they exist, and the grandparents' will otherwise, as becomes clear from Fig. 5(d). The parents' influence was found to be negligible throughout. The different orbit generations lead to slopes and spacings of the maxima that do not match along the generation boundaries. This is the origin of the observed dislocations which occur, indeed, close to the bifurcation lines.

In the full calculation with over 60 orbits, the various families with their bifurcation structures (gray lines in Fig. 2b) are superimposed. Only those dislocations survive for which the above model scenario is locally dominating and no further orbits interfere. As a result, some of the dislocations disappear, some are slightly shifted in the (s_d, B) plane, and no unique one-to-one relation between dislocations and bifurcations can be established. Nevertheless, the qualitative pattern remains the same.

In summary, our semiclassical description successfully reproduces all main features observed experimentally in the magnetoconductance of a mesoscopic channel with antidots. We have analyzed especially the dislocations of the conductance maxima as functions of magnetic field B and antidot diameter s_d , and show that these are related to bifurcations of the leading classical periodic orbits of the system. The dislocations are due to the fact that the bifurcations define the border lines between regimes of different predominant orbit generations, leading to different dependences of the conductance maxima on B and s_d . This induces the observed dislocations of the maximum positions, analogously to lattice defects at interfaces. As the classical dynamics are not affected by a rescaling of the system, the scaling behavior of the dislocations can be easily understood in the semiclassical approach.

The main mechanism for generating the dislocations has been demonstrated for 7 model orbits forming three generations related through two bifurcations, whereby the middle generation is least influential. For individual orbits, a uniform semiclassical treatment of the bifurcations is essential. For the total contribution of over 60 orbits, some cancellations take place and a convolution of the trace formula (1) over B was found to be sufficient.

The ways in which the orbit bifurcations affect the quantum oscillations here is quite different from those reported in Refs. [12–14]. There the relevant bifurcations lead to period doublings, whereas here the periods of all relevant orbits are approximately constant. Furthermore, in the RTD only a few orbits were found to be important, whereas the present system is dominated by

a much larger number of orbits with nearly identical actions, periods and amplitudes. It is not a local enhancement of the amplitudes of isolated bifurcating orbits, but the occasional mismatch of the slowly varying contributions from competing orbit generations under the variation of the system parameters that causes the dislocations in the phase plots of the conductance maxima.

We thank A. Sachraida, C. Gould and P. J. Kelly for providing us with the experimental data and helpful comments, and S. Tomsovic for a critical discussion.

- [1] M. C. Gutzwiller, *J. Math. Phys.* **12**, 343 (1971).
- [2] V. M. Strutinsky *et al.*, *Z. Phys. A* **283**, 269 (1977).
- [3] S. C. Creagh and R. G. Littlejohn, *Phys. Rev. A* **44**, 836 (1990); *J. Phys. A* **25**, 1643 (1991).
- [4] M. Brack and R. K. Bhaduri, *Semiclassical Physics*, Frontiers in Physics Vol. 96 (Addison-Wesley, Reading, 1997).
- [5] K. Richter, *Europhys. Lett.* **29**, 7 (1995).
- [6] G. Hackenbroich and F. von Oppen, *Z. Phys. B* **97**, 157 (1995); *Europhys. Lett.* **29**, 151 (1995).
- [7] K. Richter, D. Ullmo, and R. A. Jalabert, *Phys. Rep.* **276**, 1 (1996).
- [8] K. Tanaka, *Ann. Phys.* **268**, 31 (1998).
- [9] D. Weiss *et al.*, *Phys. Rev. Lett.* **70**, 4118 (1993).
- [10] A. Lorke *et al.*, *Phys. Rev. B* **44**, 3447 (1991).
- [11] S. M. Reimann *et al.*, *Z. Phys. B* **101**, 377 (1996).
- [12] D. S. Saraga and T. S. Monteiro, *Phys. Rev. Lett.* **81**, 5796 (1998); E. E. Narimanov and A. D. Stone, *Phys. Rev. Lett.* **80**, 49 (1998); and further Refs. cited therein.
- [13] K. Arita, A. Sugita and K. Matsuyanagi, *Prog. Theor. Phys. (Japan)* **100**, 1223 (1998), and earlier Refs. therein.
- [14] A. G. Magner *et al.*, *Prog. Theor. Phys. (Japan)* (1999), in print.
- [15] A. M. Ozorio de Almeida and J. H. Hannay, *J. Phys. A* **20**, 5873 (1987).
- [16] M. Sieber, *J. Phys. A* **29**, 4715 (1996); H. Schomerus and M. Sieber, *J. Phys. A* **30**, 4537 (1997); M. Sieber and H. Schomerus, *J. Phys. A* **31**, 165 (1998).
- [17] The two most important cases are $\delta = 1/6$ for tangent bifurcations and $\delta = 1/4$ for period-doubling bifurcations.
- [18] For codimension-two bifurcations, see H. Schomerus, *J. Phys. A* **31**, 4167 (1998).
- [19] C. Gould *et al.*, *Phys. Rev. B* **51**, 11213 (1995).
- [20] C. Gould *et al.*, *Can. J. Phys.* **74**, S207 (1996).
- [21] G. Kirczenov *et al.*, *Phys. Rev. B* **56**, 7503 (1997).
- [22] B. Eckhardt and D. Wintgen, *J. Phys. A* **24**, 4335 (1991).
- [23] Leading-order orbits in \hbar need not dominate alone the quantum oscillations, as pointed out for the equilateral triangular billiard [4] where an isolated orbit of relative order $\hbar^{1/2}$ is not negligible. Similarly, for the circle billiard in a magnetic field, skipping and cyclotron orbits of different orders in \hbar give comparable contributions [24].
- [24] J. Blaschke and M. Brack, *Phys. Rev. A* **56**, 182 (1997).
- [25] That a correct uniform treatment of bifurcations is not so crucial if many orbits are included, has also been observed in the disk billiard, see J. Blaschke and M. Brack, *Physica E* **1**, 288 (1997).